

Oxygen Permeation through $\text{La}_{0.4}\text{Sr}_{0.6}\text{Co}_{0.2}\text{Fe}_{0.8}\text{O}_{3-\delta}$ Membrane

Chu-sheng Chen,* Zhan-ping Zhang, Guo-sun Jiang, Chuan-gang Fan, and Wei Liu

Laboratory of Internal Friction and Defect in the Solids, Department of Materials Science and Engineering, University of Science and Technology of China, Hefei, Anhui 230026, P.R. China

Henny J. M. Bouwmeester*

Laboratory for Inorganic Materials Science, Faculty of Chemical Technology, University of Twente, P.O.Box 217, 7500AE, Enschede, The Netherlands

Received October 10, 2000. Revised Manuscript Received June 8, 2001

Dense $\text{La}_{0.4}\text{Sr}_{0.6}\text{Co}_{0.2}\text{Fe}_{0.8}\text{O}_{3-\delta}$ oxygen-permeable membranes of different thickness were prepared by solid-state reaction. The oxygen flux facilitated by an oxygen partial pressure difference across the oxide membrane was measured at elevated temperatures. It is revealed that oxygen permeation flux is entirely controlled by the transport of oxide ions in the bulk of the membrane in the thickness range of 1.25–2.46 mm. When the thickness is decreased to 0.62 mm, it becomes jointly controlled by the oxygen exchange across the gas and solid interfaces. An electrochemical approach is adopted to analyze the thickness dependence of the oxygen flux. It is shown that the interfacial process is more sensitive to the change of temperature, as evidenced by the larger activation energy for the surface oxygen exchange ($188.2 \pm 2.2 \text{ kJ mol}^{-1}$), than that for the bulk transport ($93.7 \pm 1.7 \text{ kJ mol}^{-1}$).

I. Introduction

Mixed oxygen-ion and electron-conducting oxides of the perovskite-type structure are the building stones of a variety of high-temperature electrochemical devices.¹ Among the mixed conducting oxides, $\text{La}_{1-x}\text{Sr}_x\text{Co}_{1-y}\text{Fe}_y\text{O}_{3-\delta}$ (LSCF) is found to possess appreciable oxygen permeability and reasonable stability at elevated temperatures and thus may find applications in solid oxide fuel cells (SOFC),² oxygen separators,³ and reactors for synthesis gas production.⁴

When membranes made of the mixed conducting oxides are placed in an oxygen partial pressure [p_{O_2}] gradient at elevated temperatures, there results a spontaneous flow of oxygen molecules from the high to the low p_{O_2} side.⁵ In this process, oxygen molecules are reduced to oxide ions at the membrane surface in contact with high p_{O_2} and then transported through the oxide membrane to the low p_{O_2} side where the oxide ions are reconverted to oxygen molecules. The electrical current resulting from the transport of oxide ions is compensated internally by an electronic current, so that

neither electrode nor external circuitry is required to bring about the oxygen permeation.

It is known that for relatively thick membranes the oxygen permeation is limited by the counter-diffusion of oxide ions and electrons in the bulk of the membrane and a decrease in the thickness of membrane leads to a proportional increase in the flux. When the thickness is reduced to some point, however, the oxygen exchange at the interfaces of gas and solid phases becomes rate-limiting, so that further reduction in the membrane's thickness cannot result in a significant increase in the flux. Although many studies have been conducted on LSCF,^{2–8} the oxygen transport kinetics in terms of the rate-limiting step remains unclear. This work was intended to study it by examining the dependence of oxygen permeation flux on the membrane thickness.

II. Experimental Procedures

(1) Sample Preparation. $\text{La}_{0.4}\text{Sr}_{0.6}\text{Co}_{0.2}\text{Fe}_{0.8}\text{O}_{3-\delta}$ powders were prepared by solid-state reaction. Mixtures of La_2O_3 (A.R.), CoO (A.R.), Fe_2O_3 (C.P.), and SrCO_3 (A.R.) in desired ratios were calcined in air at 850 °C for 8 h, 900 °C for 10 h, and 1060 °C for 10 h, with intermediate grinding, and then calcined at 1270 °C for 10 h using both heating and cooling rates of 1 °C/min.

Dense compacts of LSCF were prepared by uniaxially pressing powders at 350 MPa, followed by sintering at 1250

* To whom correspondence should be addressed. Fax: +86-551-3631760. Tel: +86-551-3602940. E-mail: ccs@ustc.edu.cn.

(1) Anderson, H. U. *Solid State Ionics* **1992**, *52*, 33–41.
 (2) Tai, L.-W.; Nasrallah, M. M.; Anderson, H. U. In *Proc. 3rd Int. Symp. Solid Oxide Fuel Cells*; Singhal, S. C., Iwahara, H., Eds.; Electrochemical Society: Pennington, NJ, 1994; pp 241–51.
 (3) Miura, N.; Okamoto, Y.; Tamaki, J.; Morinaga, K.; Yamazoe, N. *Solid State Ionics* **1995**, *79*, 195–200.
 (4) Tsai, C.-Y.; Ma, Y. H.; Moser, W. R.; Dixon, A. G. *Chem. Eng. Commun.* **1995**, *134*, 107–32.
 (5) Bouwmeester, H. J. M.; Burggraaf, A. J. In *Fundamentals of Inorganic Membrane Science and Technology*; Burggraaf, A. J., Cot, L., Eds.; Elsevier: Amsterdam, 1996; pp 435–528.

(6) Carter, S.; Selcuk, A.; Chater, J.; Kajda, R. J.; Kilner, J. A.; Steele, B. C. H. *Solid State Ionics* **1992**, *53–56*, 597–605.

(7) Weber, W. J.; Stevenson, J. W.; Armstrong, T. R.; Pederson, L. R. In *Mater. Res. Soc. Symp. Proc., Solid State Ionics IV*; Nazri, G.-A., Taraccon, J.-M., Schreiber, M. S., Eds.; Materials Research Society: Pittsburgh, PA, 1995; Vol. 369, pp 395–400.

(8) (a) Tai, L.-W.; Nasrallah, M. M.; Anderson, H. U.; Sparlin, D. M.; Sehlin, S. R. *Solid State Ionics* **1995**, *76*, 259–71; (b) 273–83.

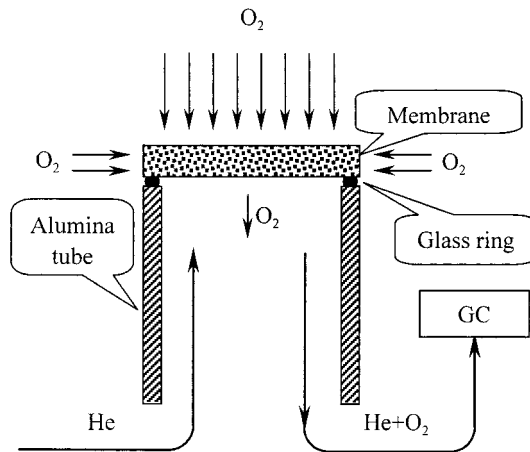


Figure 1. Schematic representation of membrane-based permeation cell.

°C in air for 10 h using both heating and cooling rates of 2 °C/min. The densities of the sintered compacts exceeded 92% of the theoretical value. The compacts were machined to disk-shaped specimens of different thickness.

(2) Oxygen Permeation Measurements. Oxygen permeation experiments were performed with disk-shaped specimens of different thickness and a diameter of 12 mm. The disks were sealed to an alumina tube using a glass ring at 900–950 °C to form a permeation cell (Figure 1). Oxygen permeation measurements were performed by exposing one side of the sealed membranes to flowing air of $p_{O_2} = 0.209$ atm and sweeping the other side with high purity helium at a rate of 10 sccm. The composition of the effluent helium stream was analyzed with a Varion 3400 gas chromatograph. In case of the occurrence of the mechanical leakage as revealed by the presence of nitrogen in the effluent, by assuming the leaked gas has the same composition as the feed gas (air), the concentration of the permeated oxygen, $C_{O_2}^{perm}$, is derived

$$C_{O_2}^{perm} = C_{O_2} - 21/79 * C_{N_2} \quad (1)$$

where C_{O_2} and C_{N_2} are the oxygen and nitrogen concentration at the permeate side, respectively. The extent of the leakage can be characterized by $1 - C_{O_2}^{perm}/C_{O_2}$, which was less than 5% in this study. The leakage is likely due to the partial failure of the glass sealing. The oxygen permeation flux corrected for the mechanical leakage is calculated by

$$J_{O_2} = FC_{O_2}^{perm} A^{-1} \quad (2)$$

where F is the flow rate at the outlet of the permeation cell and A the surface area at the low p_{O_2} side of the membranes.

III. Results

The oxygen permeation flux through dense LSCF membranes of thickness 2.46–0.62 mm are plotted in Figure 2. The oxygen partial pressure at the feed side of the permeation cell, $p_{O_2}(h)$, was kept at 0.209 atm, while at the other side the oxygen partial pressure, $p_{O_2}(l)$, was in the range 4.5×10^{-3} to 1.5×10^{-2} atm. Obviously, thinner membranes yields higher oxygen flux. An oxygen flux of 8.9×10^{-8} mol·s⁻¹·cm⁻² was observed for the 2.46 mm thick membrane at 900 °C and $p_{O_2}(l)$ of 9.3×10^{-3} atm, while 1.86×10^{-7} mol·s⁻¹·cm⁻² for the 0.62 mm thick membranes at the same temperature and $p_{O_2}(l)$ of 1.5×10^{-2} atm. The oxygen flux increases with increasing temperature, for oxygen permeation is a thermally activated process. The apparent activation energy remains almost constant of

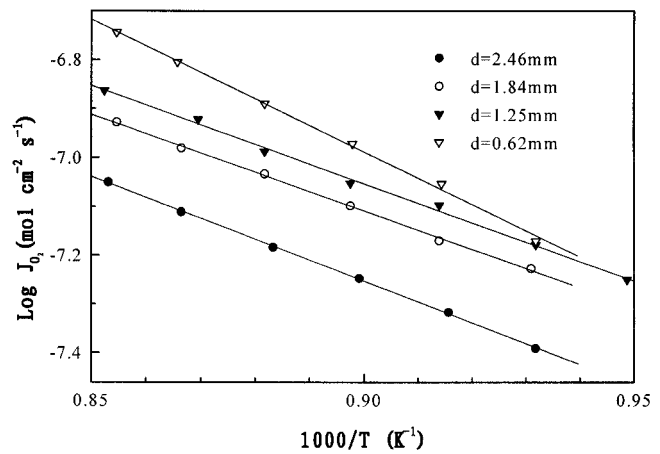


Figure 2. Temperature dependence of the oxygen permeation flux through dense LSCF membranes with different thickness.

79.8 kJ mol⁻¹ with the variation of the thickness when it is larger than 1.25 mm. When the membrane thickness is decreased to 0.62 mm, it increases to 103 kJ mol⁻¹. This indicates the change in the oxygen transport kinetics.

IV. Discussion

Oxygen permeation driven by an oxygen partial pressure difference across membranes consists of oxygen exchange at the interfaces between the gas and solid phase and counter-diffusion of oxide ions and electrons in the bulk. Corresponding to this transport scheme, a simple equivalent circuit has been proposed to identify experimentally accessible parameters which may control the oxygen flux.^{9–10} The driving force for oxygen permeation can be expressed by

$$E = \frac{RT}{4F} \ln \frac{p_{O_2}(h)}{p_{O_2}(l)} \quad (3)$$

where $p_{O_2}(h)$ and $p_{O_2}(l)$ are the oxygen partial pressure at the feed and permeate side, respectively, F is the Faraday constant, and the rest have their usual meaning.

The internal current arising from the counter-diffusion of oxide ions and electrons in the oxide membrane follows

$$i = \frac{E}{R_t} = \frac{E - \eta}{R_b} = \frac{\eta}{R_s} \quad (4)$$

where η is the driving force consumed by surface oxygen exchange, R_b and R_s are the bulk and interfacial resistance, respectively, and R_t is the total resistance ($R_t = R_b + R_s$).

The bulk resistance R_b follows

$$R_b = \frac{L}{G\sigma_{amb}} \quad (5)$$

where L is membrane thickness, σ_{amb} ambipolar conductivity, and G the factor introduced to account for the

(9) Steele, B. C. H. *Solid State Ionics* **1995**, *75*, 157–65.

(10) Chen, C. S.; Burggraaf, A. J. *J. Appl. Electrochem.* **1999**, *29*, 355–60.

Table 1. Membrane Geometry and Correcting Factor

membrane thickness (mm)	diameter at the feed side (mm)	diameter at the permeated side (mm)	correcting factor G
2.46	12.06	9.96	1.315
1.84	12.06	9.42	1.20
1.25	12.06	10.06	1.125
0.62	12.06	9.34	1.06

nonaxial transport of oxygen which arises from the fact that the side wall and edge of the membrane at the feed side all contribute to the oxygen transport (see also Figure 1). The value of G varies with the shape and the thickness of membranes and is obtained from simulation of transport in the solid using finite element method.¹¹ Table 1 lists the dimensions and values of G for samples used for permeation measurements.

Note that the internal current density is connected to the oxygen permeation flux density J_{O_2} via Faraday law:

$$i = 4F J_{\text{O}_2} \quad (6)$$

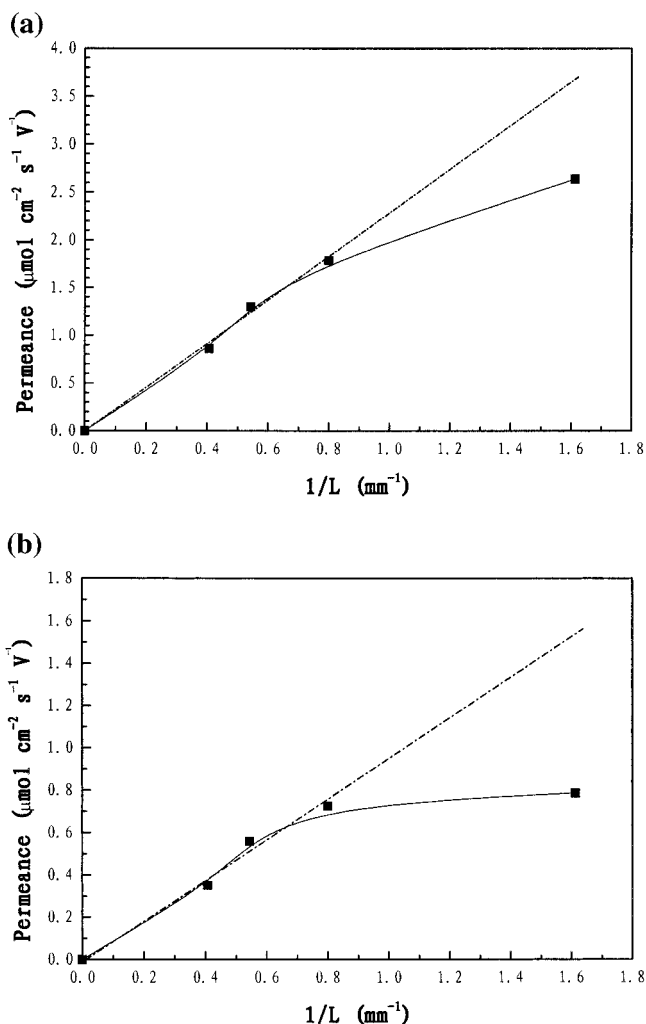
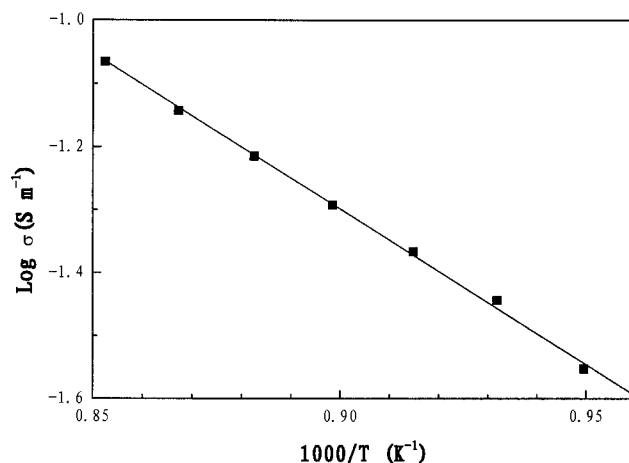
Combination of eqs 4–6 gives

$$J_{\text{O}_2} = \frac{G J_{\text{amb}}}{4FL} (E - \eta) \quad (7)$$

It is worthwhile to note that when the surface process is much faster than the bulk process, i.e., η/E is negligible, eq 7 is simplified to the one derived based on Wagner theory.^{12–13} In this case, a linear relation for $J_{\text{O}_2} E^{-1} G^{-1}$ vs $1/L$ holds, and the line passes through the origin point. The quantity $J_{\text{O}_2} E^{-1} G^{-1}$, the permeation flux normalized to the driving force and corrected for the edge effect, is equivalent to the term permeance used in the field of membrane science.

Parts a and b of Figure 3 show the permeance as a function of the reciprocal of the thickness at 800 and 900 °C, respectively. When the membrane thickness is larger than 1.25 mm, it is linear and passes through the origin. This reveals that the overall oxygen transport process is entirely controlled by the transport of oxide ions through the bulk. When the membrane thickness decreases to 0.62 mm, the oxygen permeation flux increases somewhat, but considerably less than the value extrapolated from the bulk-controlled region. This indicates that the oxygen permeation through the 0.62 mm thick dense LSCF membrane is jointly limited by the bulk transports and oxygen surface exchange. With the above-described electrochemical approach the bulk and surface processes can be further analyzed as follows.

(1) Bulk Process and Ionic Conductivity. The ambipolar conductivity of the membrane can be calculated using permeation data in the bulk controlled region of thickness 2.46–1.25 mm. For LSCF membranes, the electronic conductivity is much larger than the ionic conductivity of the oxide, so that the value of latter is virtually equal to the ambipolar conductivity. Figure 4 shows the Arrhenius plot of the oxygen ionic conductivity derived from membranes of thickness

**Figure 3.** Thickness dependence of oxygen permeance of LSCF membranes (a) 900 °C and (b) 800 °C.**Figure 4.** Temperature dependence of oxygen ionic conductivity obtained from dense LSCF membranes of thickness 2.46–1.25 mm.

The apparent activation energy E_a is calculated to be $93.7 \pm 1.7 \text{ kJ mol}^{-1}$, which is closed to that reported in the literature (92 kJ mol^{-1}).¹⁴

It should be pointed out that the oxygen ionic conductivity derived from steady oxygen permeation mea-

(11) Fan, W. B.Sc. Thesis, University of Science and Technology of China, China, 2000.

(12) Wagner, C. *Prog. Solid State Chem.* **1975**, *10*, 3–16.

(13) Lankhorst, M. H. R.; Bouwmeester, H. J. M.; Verweij, H. *J. Am. Ceram. Soc.* **1997**, *80*, 2175–98.

(14) Stevenson, J. W.; Armstrong, T. R.; Carneim, R. D.; Pederson, L. R.; Weber, W. J. *J. Electrochem. Soc.* **1996**, *143*, 2722–9.

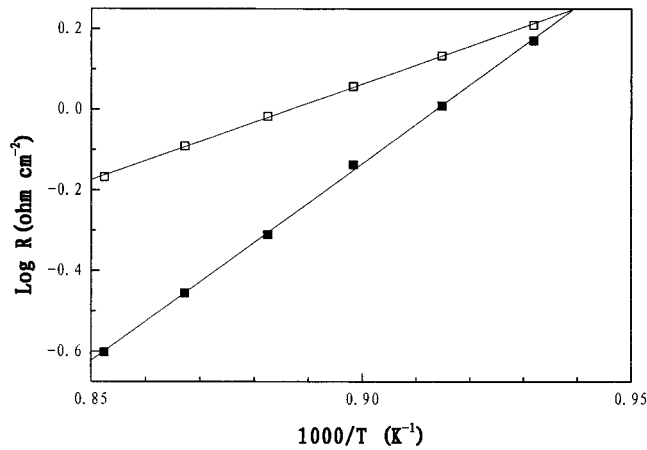


Figure 5. Temperature dependence of interfacial and bulk resistance for the 0.62 mm thick LSCF membrane: (□) bulk resistance, (■) interface resistance.

measurements is the average over oxygen partial pressure range of $P_{O_2}(h)$ to $P_{O_2}(l)$.^{5,13} In defect chemistry studies often empirical power law is used for the conductivity of oxide ions, such as, $\sigma_i(p_{O_2}) = \sigma_i^0 p_{O_2}^n$. The results of Mizusaki et al.¹⁵ show that for highly Sr-doped samples the exponent n is close to zero. Oxygen permeation measurements on the tubular LSCF membranes conducted recently in the authors' laboratory also reveal the weak oxygen pressure dependence. Therefore, for $\text{La}_{0.4}\text{Sr}_{0.6}\text{Co}_{0.2}\text{Fe}_{0.8}\text{O}_{3-\delta}$ the oxygen ionic conductivity can be regarded as independent of oxygen partial pressure and can be readily derived from oxygen permeation measurements.

(2) Surface Oxygen Exchange and Interface Resistance. For a sample with a thickness of 0.62 mm, the surface oxygen exchange starts to limit the overall oxygen permeation. This can be characterized in terms of interfacial resistance R_s , which can be calculated from

$$R_s = R_t - R_b = R_t - \frac{L}{G\sigma_{\text{amb}}} \quad (8)$$

The value of R_t is given by the ratio of the driving force (E) to the internal current density (i) as shown previously. In the present case, R_s can be readily calculated as the values for the ambipolar conductivity σ_{amb} are already derived (see Figure 4).

Figure 5 shows the Arrhenius plot of R_s for the 0.62 mm thick membrane. For comparison, the bulk resis-

tance R_b is also given. It is shown that both R_s and R_b increase with decreasing temperature. The activation energy of R_s was found to be $188.2 \pm 2.2 \text{ kJ mol}^{-1}$, which is very much larger than that of $93.7 \pm 1.7 \text{ kJ mol}^{-1}$ for the bulk resistance R_b . This means that the overall oxygen permeation is largely controlled by the surface process at low temperatures. The interfacial resistance R_s accounts for about 27% of the total resistance R_t at 900 °C and increases to 48% at 800 °C.

To evaluate the relative importance of bulk and surface transport kinetics, it is appropriate to use the concept of the characteristic membrane thickness L_c ,^{9,16} at which thickness the oxygen permeation driving force is equally consumed by the surface and bulk process, i.e., $R_s/R_t = 50\%$. When $L \gg L_c$, the oxygen flux is inversely proportional to L . When $L \ll L_c$, oxygen permeation is entirely limited by the surface process, the flux being independent of the thickness of the membranes. In the intermediate range of thickness L , the permeation is jointly controlled by the surface and bulk processes. For a given material, L_c is a function of process parameters such as oxygen partial pressure and temperature. It follows from Figure 5 that L_c increases with decreasing temperature for LSCF membrane. The value for L_c at 800 °C should be around 0.6 mm. In this case, no appreciable gain in the oxygen flux can be obtained by fabricating thinner membranes, unless some measures are taken to promote the surface oxygen exchange at the same time.

V. Conclusions

Dense $\text{La}_{0.4}\text{Sr}_{0.6}\text{Co}_{0.2}\text{Fe}_{0.8}\text{O}_{3-\delta}$ membranes can be prepared by solid-state reaction. The membranes show good oxygen permeability at elevated temperatures. When the membrane thickness is larger than 1.25 mm, the overall oxygen permeation process is entirely limited by the transport of oxide ions in the bulk of the membrane. When the membrane thickness is reduced to 0.62 mm it becomes jointly controlled by the surface oxygen exchange and bulk transport. To further enhance the oxygen permeation flux, besides fabricating thinner membranes, some measures such as coating of membranes with catalysts should be taken to promote the surface oxygen exchange.

Acknowledgment. This work is supported by the National Science Foundation of China and National Advanced Materials Committee of China.

CM000809A

(15) Mizusaki, J.; Mima, Y.; Yamauchi, S.; Fueki, K.; Tagawa, H. *J. Solid State Chem.* **1989**, *80*, 102–11.

(16) Bouwmeester, H. J. M.; Kruidhof, H.; Burggraaf, A. J. *Solid State Ionics* **1994**, *72*, 185–94.